PCT WORLD INTELLECTUAL PROPERTY ORGANIZATION
International Bureau

INTERNATIONAL APPLICATION PUBLISHED UNDER THE PATENT COOPERATION TREATY (PCT)

(51) International Patent Classification 6 : A61B 5/00

A1

(11) International Publication Number: WO 99/38433

(43) International Publication Date: 5 August 1999 (05.08.99)

(21) International Application Number: PCT/US99/02276

(22) International Filing Date: 3 February 1999 (03.02.99)

(30) Priority Data:
60/073,580 3 February 1998 (03.02.98) US

(71) Applicant: THE BOARD OF TRUSTEES OF THE UNIVERSITY OF ILLINOIS [US/US]; 352 Henry Administration Building, 506 South Wright Street, Urbana, IL 61801 (US).

(72) Inventors: CHARBEL, Fady, T.; 1200 Monroe Avenue, River Forest, IL 60305 (US). CLARK, M., E.; 2020 Zuppke Drive, Urbana, IL 61801 (US). SADLER, Lewis; 115 Elmwood Drive, Naperville, IL 60540 (US). ALPERIN, Noam; 2645 West Greenleaf Avenue, Chicago, IL 60645–3207 (US). LOTH, Francis; 10S161 Wallace Drive, Downers Grove, IL 60516 (US). QUEK, Francis; 603 North Forest, Oak Park, IL 60302 (US). ZHAO, Meide; 844 East 33rd Street, Chicago, IL 60608–6648 (US).

(74) Agents: GAMSON, Edward, P. et al.; Welsh & Katz, Ltd., 22nd floor, 120 South Riverside Plaza, Chicago, IL 60606 (US).

(81) Designated States: AL, AM, AT, AU, AZ, BA, BB, BG, BR, BY, CA, CH, CN, CU, CZ, DE, DK, EE, ES, FI, GB, GE, GH, GM, HR, HU, ID, IL, IS, JP, KE, KG, KP, KR, KZ, LC, LK, LR, LS, LT, LU, LV, MD, MG, MK, MN, MW, MX, NO, NZ, PL, PT, RO, RU, SD, SE, SG, SI, SK, SL, TJ, TM, TR, TT, UA, UG, UZ, VN, YU, ZW, ARIPO patent (GH, GM, KE, LS, MW, SD, SZ, UG, ZW), Eurasian patent (AM, AZ, BY, KG, KZ, MD, RU, TJ, TM), European patent (AT, BE, CH, CY, DE, DK, ES, FI, FR, GB, GR, IE, IT, LU, MC, NL, PT, SE), OAPI patent (BF, BJ, CF, CG, CI, CM, GA, GN, GW, ML, MR, NE, SN, TD, TG).

Published
With international search report.
Before the expiration of the time limit for amending the claims and to be republished in the event of the receipt of amendments.

(54) Title: CEREBRAL CIRCULATION MODEL AND APPLICATIONS

(57) Abstract

A method and apparatus are provided for modeling cerebral circulation in a living subject. The method includes the steps (200) of developing a model for living subjects in general, and correcting the model to substantially conform to the overall cerebral physiology of the living subject. The method further includes the step of calculating a cerebral flow of the living subject based upon the corrected model and a selected cerebral blood flow pertubation.

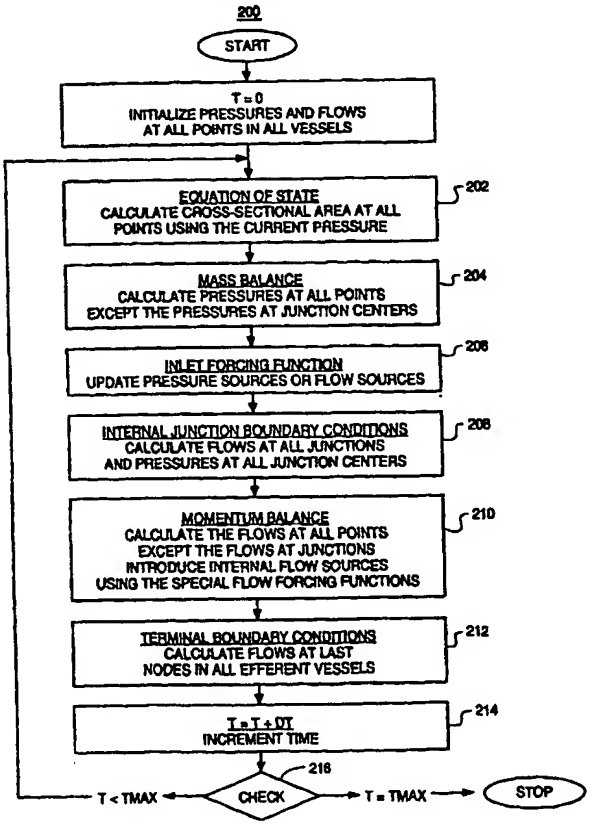

FOR THE PURPOSES OF INFORMATION ONLY

Codes used to identify States party to the PCT on the front pages of pamphlets publishing international applications under the PCT.

AL	Albania
AM	Armenia
AT	Austria
AU	Australia
AZ	Azerbaijan
BA	Bosnia and Herzegovina
BB	Barbados
BE	Belgium
BF	Burkina Faso
BG	Bulgaria
BJ	Benin
BR	Brazil
BY	Belarus
CA	Canada
CF	Central African Republic
CG	Congo
CH	Switzerland
CI	Côte d'Ivoire
CM	Cameroon
CN	China
CU	Cuba
CZ	Czech Republic
DE	Germany
DK	Denmark
EE	Estonia
ES	Spain
FI	Finland
FR	France
GA	Gabon
GB	United Kingdom
GE	Georgia
GH	Ghana
GN	Guinea
GR	Greece
HU	Hungary
IE	Ireland
IL	Israel
IS	Iceland
IT	Italy
JP	Japan
KE	Kenya
KG	Kyrgyzstan
KP	Democratic People's Republic of Korea
KR	Republic of Korea
KZ	Kazakstan
LC	Saint Lucia
LI	Liechtenstein
LK	Sri Lanka
LR	Liberia
LS	Lesotho
LT	Lithuania
LU	Luxembourg
LV	Latvia
MC	Monaco
MD	Republic of Moldova
MG	Madagascar
MK	The former Yugoslav Republic of Macedonia
ML	Mali
MN	Mongolia
MR	Mauritania
MW	Malawi
MX	Mexico
NE	Niger
NL	Netherlands
NO	Norway
NZ	New Zealand
PL	Poland
PT	Portugal
RO	Romania
RU	Russian Federation
SD	Sudan
SE	Sweden
SG	Singapore
SI	Slovenia
SK	Slovakia
SN	Senegal
SZ	Swaziland
TD	Chad
TG	Togo
TJ	Tajikistan
TM	Turkmenistan
TR	Turkey
TT	Trinidad and Tobago
UA	Ukraine
UG	Uganda
US	United States of America
UZ	Uzbekistan
VN	Viet Nam
YU	Yugoslavia
ZW	Zimbabwe

CEREBRAL CIRCULATION MODEL AND APPLICATIONS

Field of the Invention

The field of the invention relates to blood circulation in the human body and more particularly, to blood flow within the human brain.

Description of the Invention

Stroke is the third leading cause of death and disability in the United States, with significant socioeconomic impact. Therapeutic options for occlusive cerebrovascular diseases include a variety of reconstructive procedures such as endarterectomy, vessel transposition, bypass, angioplasty and thrombolysis; all of which share the common goal of enhancing the cerebral circulation.

However, because of the many individual variabilities between patients, assessment of the potential merit of such procedures is difficult and has mainly relied on clinical trials involving large groups of patients over long periods of time and at staggering costs (e.g., EC-IC bypass and carotid endarterectomy studies). The ethical dilemma of randomizing a patient to an ineffective or even harmful therapy not withstanding, selection of the optimal cerebral vascular reconstructive procedure in a given patient with complex occlusive patterns remains difficult and ultimately relies on an intuitive process.

The ability to reliably simulate such procedures for any particular patient, increases the likelihood of

selecting the optimal procedure. This invention applies a computerized model of the cerebral circulation to patients with cerebrovascular diseases to simulate any of a number of procedures, thereby providing a tool for selecting the optimal procedure for any given patient. The benefit of this invention provides improved patient outcome, significant cost savings and major impact on the way cerebrovascular reconstructive procedures are performed.

Charbel et al., *2nd International Skull Base Congress, 7th Annual Meeting of the North American Skull Base Society,* (San Diego, July, 1996) discussed the applications of an earlier computerized model of the cerebral circulation in skullbase surgery. The role of computerized modeling in cerebrovascular surgery was discussed by Charbel et al. at the *11th International Congress of Neurological Surgery* (Amsterdam, July 1997). Charbel et al. discussed the use of a computerized predictor for the tolerance of carotid artery sacrifice at *11th International Congress of Neurological Surgery* (Amsterdam, July 1997). Applications of modeling to cerebral revascularization are also contemplated.

Summary

A method and apparatus are provided for modeling cerebral circulation in a living subject. The method includes the steps of developing a model for living subjects in general and correcting the model to substantially conform to the overall cerebral physiology of the living subject. The method further includes the step of calculating a cerebral flow of the living

subject based upon the corrected model and a selected cerebral blood flow perturbation.

Brief Description of the Drawings

FIG. 1 is a block diagram of a modeling system for cerebral circulation in accordance with an illustrated embodiment of the invention;

FIG. 2 is a cerebral model used by the system of FIG. 1;

FIG. 3 is an operator interface used by the system of FIG. 1;

FIG. 4 is a flow diagram used by the operator interface of FIG. 3;

FIG. 5 is an operator display use by the system of FIG. 1;

FIG. 6 is a flow chart of cerebral modeling of the system of FIG. 1; and

FIG. 7 depicts the operator interface of FIG. 3 as it may appear during use.

Detailed Description of a Illustrated Embodiment

The present invention is a practical integration of several aspects of cerebrovascular and computer research. A program has been developed for computer aided neurovascular analysis and simulation that is useful for assessment and prediction of cerebral circulation. The program has up to four major components: (i) a vessel extraction system from Digital Subtraction Angiography (DSA); (ii) a three-dimensional phase contrast Magnetic Resonance (MR) flow measurement system and three-dimensional pulsatility visualization; (iii) a computer simulation system for cerebral

circulation; and (iv) a worldwide web-based interface and window to the world.

The process involved in the present invention creates a virtual replica of the Circle of Willis and computes network blood flow. The modeling program also allows analysis and simulation of flow and pressure within the cerebrum under the condition of a selected blood flow perturbation (e.g., a cerebral aneurysm, stenosis, bypass, other cerebrovascular disease, etc.). The modeling program currently uses the finite difference method.

The vessel extraction system is used for determining exact vessel diameters for use in the model. Currently an Attention-Based Model (AIM) forms the basis of the vessel extraction system. The vessel extraction system provides accurate and rapid measurement of vessel diameters and length at various predetermined regions of the Circle of Willis. The data with the smallest vessel size resolution (on the order of a few hundred microns) is currently derived from x-ray angiograms [platform: SGI Workstation, IRIS 6.2 Varsity Package (Rapidapp, Open Inventor, C++)].

The use of digital x-ray angiography and computerized acquisition of the digitized picture, for example through an "image-grabber" can accelerate and enhance the data acquisition process over manual reading of vessel diameters from the x-ray angiogram. The two-dimensional nature of current x-ray angiographic measurements limits the ability to derive detailed three-dimensional data from the technique.

Magnetic resonance imaging (MRI) has developed in such a manner that useful three-dimensional data

pertaining to vessel size and flow is obtainable. The current source of choice of data from magnetic resonance imaging uses three-dimensional phase contrast angiographic methods to measure flow [platform: SGI Workstation, IRIS 6.2 Varsity Package (Rapidapp, Open Inventor, C++)]. On its own, the vessel size resolution of the MRI data is on the order of a half a millimeter.

The use of this data in the three-dimensional phase contrast magnetic resonance (MR) flow measurement system of the invention enhances the accuracy of the cross-section and flow measurements by three-dimensional localization and visualization of the vessels.

Turning now to image processing, AIM will now be discussed. For the interactive approach described herein to be effective, it must exploit the facility of humans to operate or communicate within the bounds of certain rules which govern the approach. As will become apparent, AIM is a selective attention-inspired interaction paradigm for the analysis of multimodal medical images (e.g., magnetic resonance angiography (MRA), magnetic resonance imaging (MRI), xenon computed tomography (XeCT), x-ray angiograms (XRA), etc.). In general, the AIM approach exploits the strengths of both humans and machines to overcome the others' weaknesses.

FIG. 1 is a block diagram of a cerebral modeling system 10, generally in accordance with an illustrated embodiment of the invention. The modeling system 10 generally includes a data source, 12, a central processing unit (CPU) 14, a display 18 and a keyboard 16. The data source 12 may one or more medical imaging systems (e.g., MRA, MRI, XeCT, XRA, etc.).

While many aspects of human attention are yet to be ascertained, the following is known: 1. Attention facilitates the direction of limited cognitive resources; 2. Spatial cues (or prompts) are effective in directing the attentional "spotlight" for recognition; 3. Central semantic cues at both the feature and object levels facilitate performance in visual attention tasks; and 4. A model of what is in the attentional space of one's interlocutor is critical to maintaining effective communication.

AIM defines two interaction channels: a semantic context (*what* to look for) and a focus-of-attention *FOA* (*where* to look). In an AIM system 10, the user selects the context from a menu (or a schematic diagram of the neurovascular system) and manipulates a FOA cursor (*FOAC*) through the data using a 2D or 3D pointing device. For example, FIG. 2 shows the human Circle of Willis 100, including, seventy-three blood vessels. Selection of one of the vessels provides the system 10 with a context of what to look for.

FIG. 3 shows an interactive screen 152 that may be presented on the display 18 of the system 10. The Circle of Willis 100 of FIG. 2 may be displayed as a graphical context representation in a box 152 of the screen 150. An operator (not shown) of the system 10 may select a vessel (e.g., 102) using the cursor 162.

Once a context has been selected in the first box 152, the operator may show the CPU 16 where to look for the vessel in the image work area 154. The operator may identify the vessel 102 by placing the FOAC (i.e., the smart cursor 162) over the vessel and activating an ENTER button.

The AIMS processes the data in the region of the FOAC to locate and highlight entities matching the selected *context* in real-time as the cursor moves. When the correct entity is highlighted in the work area 154, the user *acknowledges* this and the system *extends the dialog* by tracing the entity (e.g., the highlighted vessel), all the while providing feedback via animated highlighting. The system may trace the entity by looking for high contrast areas between adjacent pixels or groups of pixels of the image. The high contrast areas may be used to identify boundary areas between vessels and surrounding tissue. Where the vessel is identified to the system by the operator, the system identifies the vessel within the FOAC and begins processing adjacent areas to trace the contrasted areas in three-dimensional space using the continuity of the contrasted area of a path to other parts (e.g., the respective ends) of the vessel.

Using the contrast, the system not only traces the vessel, but also measures a diameter of the vessel. The system identifies the outer wall of the vessel by seeking the area of the greatest rate of change in contrast. A measurement may then be taken of the distance between opposing sides of the vessel.

Since the system knows what it is looking for, the problem becomes one of detection of a specific entity. Hence, very specifically tuned detectors may be used. It is not critical if the detector highlights the wrong entity because the user can retarget the detector by simply moving the pointing device.

AIM defines an abstraction hierarchy of *contexts*. A *context* may vary in abstraction from full scene

interpretation through object level, feature level and point level *contexts*. In the domain of neurovascular tree, an object level context may be a segment of the carotid artery, a feature level context may be arterial boundary model, and in the point level context, a user may trace the boundary points of a vessel by hand. This provides robustness for the system for our mission-critical task in the process of patient care. For neurovascular image interpretation, this guarantees the ability to obtain the necessary vessel extraction and measurement even if the higher-level recognition algorithms fail (e.g., owing to patient pathology or data quality).

The AIM model provides a system and software architecture of broad applicability. This is important because *AIMS* is easily extensible to accommodate new algorithms, imaging modalities and entities of interest (e.g., other brain structures such as the interhemispheric chasm of the brain, aorta walls for cardiovascular image interpretation, tumor models for digital mammogram analysis) without requiring extensive ad hoc reengineering for each domain. FIG. 4 is a block diagram of the architecture characterizing the interaction model. The object-oriented architecture comprises two distinct components: The user interface and the domain knowledge representation. Such modularity is important for the system 10 to be portable across platforms and display/interaction technologies (e.g., for both 2D and 3D interpretation environments).

The *context database* maintains domain knowledge about the entities of interest (e.g., vessels of different types, and the operators necessary to extract

them from the different kinds of image data). The *data information* maintains meta-information about the data (e.g., file name sequences, where data is stored, the resolution of each image type, etc.). The *Operator Selector* selects the appropriate FOAC operator from the *Operator Library*. The *Process knowledge database* maintains knowledge of the interpretation protocol.

The *process knowledge database* realizes the concept of *dialog extension* by tying it directly to medical/radiological protocol. For example, in the domain of neurovascular image interpretation, the protocol dictates an order of vessel extraction that is efficient with respect to the ordering of the XRA dataset and the content of particular viewing projections in the XRA images. This protocol can be encoded seamlessly into the interaction sequence so that the system prompts the user for each succeeding vessel in the neurovasculature. A *protocol definition file* pairs the order of vascular measurement with the preferred images in which the measurement may be made. The system may simulate an extended dialog by prompting the user for each vessel measurement in the appropriate images. This permits the system to predict the next entity to be extracted so that the user does not have to remember the order thus reducing processing errors (e.g., missing or mixed-up readings). This example also illustrates the concept of interrupting and resuming dialog streams. A user may wish to interrupt the protocol for several reasons. She may wish to correct and erroneous measurement made earlier, or may want to make a measurement of opportunity out of sequence. *AIM* permits such interruption by having the user select the

context of interest. One may think of this as the user "changing the subject". *AIM* maintains the location of "interrupt on" and permits the user to resume the dialog (or protocol) whenever she wishes. Hence, the *process knowledge database* actually facilitates the psycholinguistic components of discourse situatedness and repair that are essential for effective interaction.

FIG. 3 shows the general screen layout of the AIM interface 150 used in the interpretation of complex images. The *Working Area* 154 is the primary area in which the operator interacts with the system in the interpretation task. The *Focus of Attention* (*FOA*) is directed by manipulating the *Smart Cursor* 162 over the displayed subject image in the *Working Area* with a pointing device (e.g., a mouse). Feedback for the interpretation process is provided in the *Working Area* by highlighting the objects under the *Smart Cursor* which satisfy the current context. The *FOA Status Display* 158 at the bottom left of the display provides a magnified view of the area under the *smart cursor* as well as the processing status. In a later section, we shall see how partial processing results are presented in this display.

The *Graphical Context Presentation* 152 on the left side of the screen provides the user with the overall status of the interaction as well as the particular interpretive *context*. In our neurovascular interpretation prototype, this is a schematic of the neurovascular tree. In a cardiovascular measurement system, this may be a schematic representation of the aortic system. The schematic representation provides the user with an overall state of the interpretation

process with the use of color (e.g., in our neurovascular measurement system of the context box 152, already measured vessels are filled with green, and *context* vessel is colored red). The user may interrupt the dialog process (or measurement protocol) by selecting a *context* object in this window by direct selection of its representation in this schematic. In addition to this graphical presentation, this generic screen layout also provides for textual context identification in the *System Status* and *Process Status* boxes 156, 160. The former provides general information about the selected context, and the latter details the status of the current interpretation (e.g., the dimension of the vessel being measured in the current image).

The pulldown menu items 164 on the top of the screen permit alteration of the system parameters and selection of data sets on which to operate.

Owing to the strong man-machine interaction model behind it and the *user interface design principles* used in the development of the interface, the AIM interface described herein is simple, yet effective and easy to use. FIG. 7 shows an example of the AIM interface 150 as it may appear during the interpretation of XRA images of the neurovascular system. The XRA image is displayed in the *Working Area* 154. This area is scrollable, so any size of XRA image can be displayed. The user can increase or decrease the size of the image at any time by choosing appropriate selection item from the menubar 164. The *Focus of Attention* (*FOA*) is represented by the box 162 shown in the image and is directed by the mouse. A schematic representation 100 of the neurovasculature

is provided in the *Graphical Context Presentation* 152. It is shown in the upper left corner of the screen to provide object level context to the system in a graphical fashion. When the user selects a vessel on this schematic representation 100 (using the mouse), the information about this vessel is displayed in the window 160 in the lower right corner of the screen. This information contains the vessel number (used as an index), the vessel name, the width and any comment written by the user about the measurement process of this vessel. If no measurement has been taken for this vessel, the vessel, the vessel has the default width stored in the database. The vessels are highlighted in different colors to give feedback on the selection and measurement processes.

The *FOA Status Display* 158 at the bottom left of the screen displays the processing status of the smart cursor. It shows a magnified view of vessel boundary found in the *FOA* and locates the cross-section where the measurement is being made. Partial results of the computation and the process parameters are also shown in this area.

The *AIM* neurovascular measurement system is designed to be used by medical/radiological personnel. Hence, it is advantageous to exploit the familiarity of such experts with systems they currently use for the selection of XRAs to be used in the measurement. FIG. 5 shows an additional window 177 that facilitates the easy use of the system 10. In the system 10, every patient's XRA images are stored on the storage device in a separated directory. The system 10 creates thumbnail images of the original images, as shown in the window

177, which are 128x128 and 256x256 pixels wide. The user can see all of the 128x128 versions of the thumbnail images at the same time on a window similar to the lightboard used by the doctors to inspect the XRAs. When the cursor 162 is held on one of the thumbnail images for a few seconds, the bigger, 256x256 version of theta image is displayed on the screen. This allows the user to inspect the image more carefully. When the user decides to choose one image for interpretation, he simply clicks the mouse button and the system brings the original version of this image into the *Working Area*. Another important feature of the system is that the interpretation process is done in real time on modest computation hardware. Instead of processing the entire image, only the area under the FOA is processed, resulting in very fast processing speeds. The strong feedback mechanisms, both graphical and textual, during the interpretation process make the system effective and easy to use.

A practical system for neurovascular interpretation must account for different individuals doing the measurement and using the measurement result. A surgeon may delegate the measurement process to a medical technician, but the surgeon is ultimately responsible for her final treatment decision. Hence, the *AIM* dialog model has been extended to include the recording of the state of the interaction when the measurement was acquired. This *History of Measurement* feature maintains information about the measured vessels, including identifier of the image used, the coordinates and size of the FOA at the point of measurement. The measurement results are stored in a database for every measurement

taken. This permits the physician to perform "quality control" checks of the measurement. Any measurement status may be recalled by selecting the vessel on the schematic representation or from the measurement table at the bottom right of the screen (the *Process Status* window). The user may also step through the measurement and quality control, the user can change any measurement taken using the *AIM* interpretation process.

As described above, vessel size and location may be obtained from MRA, MRI, XeCT or XRA data. The dimensional information derived from the data may be enhanced using MRI operating in the Doppler mode. The use of Doppler MRI allows volumetric blood flow to be determined by measuring blood velocity across a cross-section of each vessel.

The enhancement of the accuracy and vessel size resolution arises from the three-dimensional reconstruction of the vessels that currently uses an interpolation scheme that is constrained by a piecewise smooth volumetric flow equation. The flow data is corroborated by transcranial Doppler measurements at predetermined vessel intervals. The flow velocity has also been found to vary as a result of vasoreactivity. Benchmark values for cerebral autoregulation have been established and is continuously refined.

The data analysis system supports both automatic and interactive extraction of the vessel cross-sections. A color coding scheme facilitates visualization and user interaction with the data to reduce the inter-user variability.

For example, a user can view, move and freely rotate a three-dimensional picture of the

cerebrovascular network 100. The user can also place a plane anywhere in the three-dimensional picture, then view the two-dimensional cross-section of the cerebrovascular network 100 at that location.

The vessels are clearly discernible in the cross-section, with color coding to denote flow into and out of the planar cross-section. Three-dimensional pulsatility of blood flow can be animated and visualized in the currently-developed user interface 150. A vessel can be selected by the user for detailed and graphical analysis of the flow through the vessel cross-section that animatedly shows the pulsatile flow changes with time.

The computer simulation system 10 for cerebral circulation employs the outputs from both the vessel extraction system and the three-dimensional phase contrast MR flow measurement system to calibrate, customize and drive the cerebral circulation model [platform: PC (Pentium), Windows95/NT or DOS, Lahey Fortran 77]. The model is reconfigurable to account for person-to-person variability in the cerebrovascular network. The overall number of vascular segments in the flow model can be increased or decreased as needed to form a customized model for each patient.

The computer simulation system is flexible and accommodates empirical observations of measurements from the x-ray and magnetic resonance angiograms as well as from direct measurements of flow using flowmeters during surgery, and transcranial Doppler (TCD) at selected sites. The parameters of the model can be adapted as validation of the model requires in "normal" subjects and subjects with cerebrovascular diseases.

The computer model is a one-dimensional, explicit, finite difference algorithm based on a conservation of mass equation, a Navier-Stokes momentum equation, and an equation of state relating local pressure to local size of artery [Khufahl & Clark, *ASME J. of Biomech. Eng.* **107**:112-122 (1985)].

Since the arterial networks contain vessel loops (as well as many branchings), the pressure and flow nodes are staggered throughout the model. Each vessel is divided into many segments; the flow nodes are located at segment ends, the pressure nodes at segment centers. Any multi-vessel network configuration can be specified solely from the data file.

The model is forced by one or more pressure or flow signatures at appropriate locations. Usually, a pressure-time signature at the root of the aorta, obtained from prototype measurements or angiographic data, serves as the forcing function. Velocities at certain points in the network as determined by transcranial Doppler measurement are also integrated.

As shown (FIG. 6), the model of the system 10 is first initialized 202 with initialized pressures and flows at all points in all vessels. A cross-sectional area is calculated 202 for all points using the current pressure. The mass balance is determined 204 by calculating pressures at all points except the pressures at vessel junction centers. An inlet forcing function is invoked 206 to update pressure and flow sources. The internal junction boundary conditions may be evaluated 208 by calculating flows at all junctions and the pressures at all junction centers.

A momentum balance may then be determined 210 by calculating the flows at all points except the flows at junctions. The pressures at all junction centers may be used as special forcing functions to introduce internal flow sources. A set of terminal boundary conditions may be determined 212 by calculating flows at the last nodes in all efferent vessels.

Finally, a current time value is incremented 214 and the incremented time is compared 216 with a modeling period. If the incremented time is less than the modeling period, the process 200 repeats. If not, the process terminates.

A baseline vessel network 100 is used in the current model, including the Circle of Willis, ophthalmic arteries and other natural anastomoses. When surgical anastomoses are considered, the number of vessels can rise as needed. In addition, segments stenosed (perturbed) by any specified amount can be placed in any number of vessels. Aneurysms can also be simulated at various sites in the network. The results of any of a number of surgical procedures may be accurately predicted based upon the model results of the system 10.

A worldwide web-based interface and window to the world is available to allow users access to the interactive and user-friendly program from remote sites throughout the Internet.

The system for computer aided neurovascular analysis and simulation is usefully applied to model and analyze various neurosurgical conditions.

Early models of blood flow in the brain were based upon an assumption that any particular artery feeds a

particular part of the brain. The volume of brain fed can be calculated. First, the total mass of the brain can be determined. Then, the portion fed can be determined as a percentage of the determined total. Knowing the mass of brain fed by a particular artery allows the volume of blood necessary to feed that mass to be determined. Those early models were general, using assumptions of the elasticity of the blood vessels, the viscosity of the blood, and the vasculature arrangement of a normal patient's brain circulatory system.

The present invention is a refined model that is capable of being adapted to specific patients. Once the volume of blood necessary has been determined, the model is calibrated to a particular patient.

Deviations of the arterial structure of the blood supply of the patient's brain from the general model are identified from the angiograms. An x-ray angiogram (XR angiogram)of the patient's brain is used to determine the diameter of the blood vessels. Phase contrast Magnetic Resonance imaging angiography (MR angiography) is then used to determine an actual blood flow in the brain. Missing or additional arterial segments may be identified and used to adjust the model. A knowledge of the actual arterial structure and actual blood flows can be used to customize the model to the actual patient.

An empirical study of user variability using the three-dimensional phase contrast MR angiographic flow measurement system was conducted. The study implemented an end-to-end system. The study tested the repeatability of measurements by having ten users select the vessel cross-section from the interpolated color

velocity images of the cerebrovascular flow. The flow computation performance of the system was verified against the data collected from a constant flow phantom, from ten patients with varying cerebrovascular diseased, and from a computational fluid dynamic (CFD) simulation.

The results of the empirical study show that the readings are stable across users, and that the flow measurements show a good degree of fidelity to the flow obtained through clinical measurement and CFD simulation. A 96 percent overall accuracy on 160 measurements was observed for the phantom, with less than 5 percent mean error in the inter-user variability in extraction of the vessel cross-section among the ten users. For the ten patients, the flow computed was satisfactory in qualitative evaluation. The computed flow also correlated very well with those measured with a flowmeter in two patients $r=0.985$, $P<0.001$). The flow measurements in the Circle of Willis correlated well with the results of a CFD simulation of two patients ($r=0.970$, $P<0.001$).

Cerebral Circulation Modeling

The circulation around the "Circle of Willis" as first described in 1664 was initially only thought to be a poorly functioning anastomotic network at the base of the brain. Willis, *Annals of Medical History* **2**:81-94 (1940). Later it became accepted that it acts as the main distribution center for cerebral blood flow. In health, it distributes blood proportionately to each part of the brain; in disease, when the blood supply is decreased or diminished, it can redistribute flow in an effort to maintain cerebral hemodynamic homeostasis.

Because the cerebral circulation network is encased by the skull, it is very difficult to measure flow and pressure in its blood vessel constituents in a direct manner. Therefore computer simulation using the system 10 becomes an attractive way to predict flows and pressures in the cerebral circulation network. Fluid dynamic-based computer simulation offers the convenience of predicting pressures and flows at almost any desired section in the circulating system. Moreover, it not only can be used to estimate the flow and pressure under health and disease situations, but also can be used to predict the result of treatment procedures.

The simulation of cerebral circulation presents a range of challenging fluid dynamic problems, including: modeling the non-Newtonian properties of blood; dealing with "physiological" unsteady pulsatile flow; modeling the elasticity of vessel walls; and modeling moving boundaries caused by vessel wall elasticity. In addition, because the cerebral circulation network is an interconnected three dimensional arterial network, the question arises of how the curvature of the artery is modeled. The asymmetric and three dimensional characteristic of bifurcations are also very important issues.

Computer simulation started with models of the dog's cerebral circulation system. Clark et al., *Acta Neurol. Scandinav.*, **43**:189-204 (1967), built a computer model for one-dimensional, linear, steady laminar flow and compared the result with an engineering model built by the same group [Himwich et al., *Archive of Neurology*, **13**:164-172 (1965); Himwich et al., *Archive of Neurology*, **13**:173-182 (1965)]. Cooper, *Ph.D. thesis*, Washington

University (1970), studied the pulsatile flow effect. Chao & Hwang, *TiT Journal of Life Science*, **2**:3-81 (1972) simulated non-linear pulsatile flow in their model. Himwich & Clark, Pathology of Cerebral Microcirculation, J. Cervos-Navarro, ed. (Walter de Gruyter, New York: 1974), pp. 140-152, and Clark & Kufahl, Proc. of 1st Intl. Conf. Cardiovascular System Dynamics, MIT Press (Boston, 1978), pp. 380-390, simulated the pulsatile flow in distensible vessels. Hillen et al., *J. Biomechanics*, **15**:441-448 (1982), developed a non-linear, one-dimensional model, simplified to only five vessels, that accounted for pulsatile flow and elastic vessel walls. Kufahl & Clark, *J. Biomechanical Engineering*, **107**:112-122 (1985), developed a one-dimensional finite-difference model with distensible vessels. Kufahl & Clark's dog model contained thirty-five vessels, both steady flow and pulsatile flow were studied.

Beginning in the late eighties, investigators started to simulate the human cerebral circulation. Adapting the animal models to generally simulate human cerebral circulation was not trivial.

The cerebral circulation network of a human is more complex than the that of an animal. Considerations to be addressed included the number of arteries it was necessary to simulate, the selection of those arteries, and the configuration of the chosen arteries to represent the functionality of the Circle of Willis.

Cerebral circulation in humans is not consistent between individuals. The number of arteries, and parameters such as artery length and diameter differ from person to person, limiting the utility of standard data for individual cases. A successful model must be

very flexible and robust to handle various simulation conditions.

The difficulty of obtaining direct measurements in humans limits the ability to accumulate parameter information to refine the model.

Clark et al., *Neurological Res.*, **11**:217-230 (1989), developed an elaborate model for the human cerebral circulation network following the mathematical method used by Kufahl & Clark, *J. Biomechanical Engineering*, **107**:112-122 (1985). The new model included seventy-three vessels representing the basic Circle of Willis. FIG. 2 is the schematic drawing of the 73 vessel model of Clark et al. After adding naturally occurring anastomoses, the total number of vessels increased to eighty-five. When artificial anastomoses were imposed, the number of vessels increased to eighty-seven.

Duros et al., *Neurological Res.*, **13**:217-223 (1991), built a model that not only contained the cerebral arteries but also the human body main supply arteries. The Duros et al. model was used to simulate the rupture condition of aneurysm.

Beside the fluid dynamic models, several electrical models were built based on the similarity of the governing equations of electrical circuits and one-dimensional linear flow. Moreover, electrical networks are good at simulating networks with capacitance and resistance. Electrical network models are also well understood and provides convenient abstractions. Roller & Clark, *J. Biomechanics*, **2**:244-251 (1969) simulated the pulsatile flow and flexible vessel wall using transmission line theory. Hellal, *Comput. Biol. Med.*, **24**:103-118 (1994), built an electrical model using

transmission line equations derived from the linearized Navier-Stokes equation and vessel wall deformation equation.

Differences between the Existing Models.

All existing cerebral circulation models are one-dimensional. All fluid dynamic-based models are electrical models that begin with the same set of governing equations, namely the one-dimensional continuity equation and Napier-Stokes equation. In those models, the following assumptions must be made in order to derive the equations [Long et al., *J. Fluid Mech.*, **55**:493-511 (1972); Imaeda, *Ph.D. thesis*, Univ. of Waterloo (1975); Imaeda et al., *J. Biomechanics*, **13**:1007-1021 (1980); nerm et al., Handbook of Engineering (McGraw-Hill, New York: 1987), pp. 21.1-21.21]: (i) The flow is radially symmetric and well-developed laminar flow; (ii) blood is an incompressible, Newtonian fluid; and (iii) external forces (e.g. gravitational force) are negligible.

Because the most important components of interest are flow and pressure distributions, the one-dimensional integrated continuity and momentum equations are more convenient. The integrated governing equations are [Kufahl & Clark, *J. Biomechanical Engineering*, **107**:112-122 (1985); Raines et al., Proc. of the Summer Computer Simulation Conference (MIT Press, Boston: 1975), pp. 890-900; Raines et al., *J. Biomechanics*, **7**:77-91 (1974); Proenta et al., *J. Biomechanical Eng.*, **108**:161-167 (1986)]:

continuity equation:

(1) $$\frac{\partial Q}{\partial x}+\frac{\partial A}{\partial t}=0$$

momentum equation:

(2) $$\frac{\partial Q}{\partial x}+\frac{\partial\left(Q^2/A\right)}{\partial x}=-\frac{A}{P}\frac{\partial P}{\partial x}+\frac{\pi D\tau}{\rho}$$

where Q is a quantum flow and A is cross-sectional area. τ is the shear stress at the wall. The convective term

$$\frac{\partial\left(Q^2/A\right)}{\partial x}$$

makes the governing equation set nonlinear.

The main differences between the various models are how they define the problem (e.g. whether the flow is steady or pulsatile, whether the vessel wall is rigid or elastic, and whether a linear or non-linear governing equation is used to describe the flow field) and how they solve the problem (e.g. whether an analytical method or numerical method is used).

Definition of the Problem.

Even when the assumption is made that blood is Newtonian and flow is laminar, the governing equations are still non-linear because of the existence of the convective term in the momentum equation. For pipe flow, The convective term can be ignored because the gradient of the velocity is very small. The result is a linearized Navier-Stocks equation. If it is further assumed that the vessel wall is rigid and the flow is steady, the problem becomes Poiseuille flow, which can

be solved analytically by applying the well-known Hagen-Poiseuille formula.

$$Q = \frac{\pi R^2 (P_a - P_b)}{8 \mu \ell} \quad (3)$$

where R is the pipe radius and l is the pipe length.

For the rigid vessel unsteady pulsatile flow, Wormersley, *Phys. Med. Biology*, **2**:178-187 (1957), gave an analytical solution. Ling & Attack, *J. Fluid Mech.*, **55**:493-511 (1972), extended the Wormersley model by taking into account the consideration of non-linear effects and distensibility of the blood vessel. The finite difference technique was employed to solve the problem numerically. To date, most existing models can handle the non-linear, pulsatile flow and distensible vessel wall problem.

From the definition of the problem, a computer model can be divided into two categories.

The first type of models applied the linear governing equation and rigid vessel assumption. For steady flow, the solution is given by the Hagen-Poiseuille formula. For unsteady flow, the solution is given by the Wormersley model. Examples of models of this type include Clark et al. *Acta Neurol. Scandinav.*, **43**:189-204 (1967), and Hillen et al., *J. Biomechanics*, **21**:807-814 (1988). Because some of the electrical models [Roller and Clark, *J. Biomechanics*, **2**:244-251 (1969); Helal, *Comput. Bio. Med.*, **24**:103-118 (1994)] were derived from the Hagen-Poiseuille formula, they belong to this type. The advantages of a model with linear governing equation and rigid vessel assumptions

is that the model is simple and an analytical solution exists. Thus sensitivity analysis of parameters can be performed. It also offers the possibility of gaining insight into mechanisms that govern the flow in the cerebral network.

The other type is non-linear, pulsatile flow and distensible vessel models. Examples of models of this type include Kufahl & Clark [Kufahl and Clark, *J. Biomechanical Engineering*, **107**:112-122 (1985); Clark et al., *Neurological Research*, **11**:217-230 (1989); Kufahl, *Ph.D. thesis* (Univ. of Illinois, Urbana: 1980)] Hillen et al. [Hillen et al., *J. Biomechanics*, **15**:441-448 (1982); Hillen et al., *J. Biomechanics*, **19**:187-194 (1986)] and Duros et al., *Neurological Research*, **13**:217-223 (1991).

The advantage of this kind of model is that the non-linearity, pulsatile flow and distensible vessels are more accurate than the first type's in describing the physical behavior of blood flow in arteries. For instance, Ling and Attack, *J. Fluid Mechanics*, **55**:493-411 (1972), point out that the non-linear term cannot be neglected. Kufahl and Clark, *J. Biomechanical Engineering*, **107**:112-122 (1985), showed that pulsatile flow resulted in a 10 percent increase of the total flow and contributed to some flow redistribution.

Problem Solution.

For the first type of problem, analytical solutions exist. For the second type of problem, numerical techniques must be used. The most commonly used computational fluid dynamics tools are finite-difference (FD), finite-element (FE) and finite volume (FV).

In the task of simulating the human cerebral circulation system, the finite-difference technique is widely used [Kufahl & Clark, *J. Biomechanical Engineering*, **107**:112-122 (1985); Clark et al., *Neurological Research*, **111**:217-230 (1989); Duros et al., *Neurological Research*, **13**:217-223 (1991); Kufahl, *Ph.D. thesis* (Univ. of Illinois, Urbana, 1980)] because the application of finite difference approach is straightforward and it can achieve certain accuracy with modest computational resources. However the finite difference approach requires high regularity of the grid, and this restrains the approach to be used in solving complex geometry problems.

In contrast, the finite element approach can handle the complex geometry problem very easily, but the shortcoming of this method is that it needs much more computation time than the finite difference method.

Cerebral network models usually contain hundreds of arteries and tens of bifurcations, which makes the use the finite element approach difficult using presently available computer equipment. To apply the finite element method in the network simulation, powerful computers are needed. With advances in computation technology, the finite element method can be applied in cerebral network simulation. The present invention currently incorporates the finite difference approach.

Application.

Stroke is the second leading cause of death in the United States, as well as in most western countries. Among the many approaches available for cerebral revascularization (e.g. angioplasty, endarterectomy, byphase and embolectomy), the procedure of choice for

each particular patient is at least in theory the one that restores cerebral blood flow. However because of the complex architecture of cerebral circulation, each patient has a unique dimensional structure. As a result, any surgical treatment can have different effects on different patients.

Computer models can simulate the cerebral circulation under "normal" conditions. Computer models can also be used to predict the results of potential treatment procedures. However, there is no system currently available which forms a comprehensive model customized to the patient or which allows a user to perturb that model at will.

Hillen et al., *J. Biomechanics*, **15**:441-448 (1982), built a non-linear one dimensional model to study the functional significance of the Circle of Willis. The model consisted of two afferent and two efferent arteries connected by the posterior communicating artery. Hillen et al. found that in normal cases, the flow in the posterior communicating artery was towards the posterior cerebral artery, and that the flow direction in posterior communicating artery depended on the ratio of peripheral resistance. Raising the ratio significantly would change the flow direction, therefore Hillen et al. postulated the formation of a dead point where flow in the posterior communicating artery approaches zero.

Kufahl and Clark, *J. Biomechanical Engineering*, **107**:112-122 (1985), developed a 35-vessel computer model for dog circulation. The model was non-linear, one-dimensional with pulsatile flow and distensible vessel walls. The computer simulation revealed the large drop

in pressure over the length of the middle cerebral due to the large fluid friction at the vessel wall. Large pulses of flow were found in the common carotid but smaller pulses occurred farther downstream.

The comparison by Kufahl and Clark of running the model with steady flow versus pulsatile flow showed that the total rate increased as the effect of pulsatile flow. Kufahl and Clark also found flow redistribution in some arteries.

A series of stenosis were simulated by Kufahl and Clark to study the efficacy of the Circle of Willis in maintaining the flow under arterial disease. The middle cerebral flow was found to be well-maintained under different cases, including the few cases in which the pulse vanished.

Hillen et al., *J. Biomechanics*, **21**:807-814 (1988), extended their previous model [Hillen et al., *J. Biomechanics***15**:441-448 (1982)] to include 18 vessels. The effect of asymmetry on the flow distribution in afferent and efferent vessels and the possibility of the occurrence of a "dead point" in the posterior communicating artery were studied. The authors found that a slight asymmetric change in the right posterior communicating artery (doubling the diameter) could result in noticeable effects in the flow distribution (flow in the left carotid artery exceeded that in the right carotid artery, a small flow was present in the anterior communicating artery), but the pressure seemed to be unaffected. The authors pointed out that a dead point in the posterior communicating artery cannot occur in humans.

Hillen et al., *J. Biomechanics*, **21**:807-814 (1988), simplified their model by ignoring pulsatility and vessel wall elasticity. From the comparison of the simple model and the previous model, they concluded that the deletion of pulsatility and vessel wall elasticity caused only a slight decrease of the flows without any flow redistribution. This finding was in contrast to the study of Kufahl and Clark, *J. Biomechanical Engineering*, **107**:112-122 (1985), in which the flow redistribution was found due to pulsatile flow. The authors concluded the contradiction was caused by the ways in which the terminal resistances were determined in the different models. Hillen et al. used the Hagen-Poiseuille resistance, whereas Kufahl and Clark calculated energy losses from a quasi two-dimensional velocity profile that is approximated by a sixth degree polynomial.

Clark et al., *Neurological Research*, **11**:217-230 (1989), built four computer models for the human Circle of Willis. The first model contained 73 vessels ("model 73") representing the basic circle and served as a benchmark. The second model was constructed by adding the naturally-occurring secondary anastomosis, the total number of vessels increased to 85 ("model 85"). Adding an artificial anastomosis between the frontal artery and the middle cerebral artery in model 73 and model 85 resulted in model 75 and model 88, respectively.

In order to evaluate the ability of each of the anastomotic vessels under normal conditions, Clark et al. studied five cases. In each case, a slight increase in the diameter of the anastomoses was observed over the previous model. The results showed that the EC-IC

bypass was very beneficial when non natural anastomoses were present.

In another five cases, 90 percent stenosis was imposed in the middle cerebral artery. The same studies were performed by Clark et al. as before. Clark et al. found that the anastomotic channels helped supply the ischemic areas, the larger the diameter, the better the supply. And again, the artificial anastomoses were most beneficial when the natural anastomoses were not present.

Later Charbel et al. ["Predictive value of a computerized model of the cerebral circulation", *44th Annual Meeting of Congress of Neurological Surgeons* (Chicago, 1994); "Validation and clinical potential of a computerized model of the cerebral circulation", *1st Annual Meeting on the Joint Section on Cerebrovascular Surgery of the AANS & CNS* (1996)] introduced both quantitative, semi-quantitative, as well as direct quantitative methods of validating a patient-specific computer model by directly measuring flow in blood vessels during surgery and comparing the values with the computer model. More recently, the same group began utilizing magnetic resonance as another valuable validation tool, "Phase Contrast MR flow measurement system using volumetric flow constrained image interpolation and color coded image visualization", *47th Annual Meeting of Congress of Neurological Surgeons*, (New Orleans, 1997), thus further bringing computer modeling within the reach of the clinician.

Duros et al., *Neurological Research*, **13**:217-223 (1991), built a 69 vessel model to simulate the cerebral circulation with an aneurysm. The mathematical method

used in the model was the same as Kufahl and Clark, *J. Biomechanical Engineering*, **107**:112-122 (1985). The Duros model differed from the other models in that the model not only contained cerebral arteries, but also contained 30 main supply arteries to different organs of the human body.

The aneurysm was balloon-shaped, elastically tapered with zero distal flow and was placed at the junction of the internal carotid, the anterior cerebral and the middle cerebral arteries. To simulate the condition where a rupture may happen, several parameters were adjusted: all terminal vessels' resistance values were enlarged by a factor of 10; two 80 percent stenoses were placed in the middle cerebral artery and anterior cerebral artery. Systemic pressure was increased to 150 mm Hg to represent hypertension. The compliance coefficient of the aneurysm was set to 1.5 to represent a stiff wall condition.

Duros et al. focused on the pressure propagation inside the aneurysm and found that the pressure did not change with the neck diameter, but the pressure peak value increased with increasing the sack diameter. In order to achieve a high pressure (310 mm Hg) which may trigger the rupture of the aneurysm, hypertension, increased number of reflecting sites in both the near and far fields, and arteriosclerotic arteries were needed.

Computational Fluid Dynamic Modeling of Cerebral Blood Flow During Carotid Occlusion.

The surgical treatment of giant aneurysms or head and neck neoplasms often requires permanent occlusion of the internal carotid artery. Tolerance to permanent

carotid artery sacrifice is traditionally assessed by temporarily occluding the carotid artery. This procedure is not without risk. The computational model of cerebral circulation of the present invention is a safer alternative to the balloon occlusion test (BOT).

The model used by the system 10 was used to create a virtual replica of the Circle of Willis and compute network blood flow using the finite difference method. To evaluate the ability of the model to identify patients who tolerate permanent carotid occlusion, the difference in ipsilateral computed middle cerebral artery flow between patients passing and failing the balloon occlusion test was determined prospectively.

Each patient underwent four vessel angiography and awake temporary occlusion of the internal carotid artery. Failure of the BOT was defined as appearance of any one of the following: a neurological deficit during the BOT, slowing of EEG wave patterns, and a drop in RSO_2 of >10 percent.

Five of the 22 patients failed the BOT. The change in computed middle cerebral artery flow was 7 +/- 0.74 cc/min for patients passing the BOT ($p<0.001$).

The value of computational fluid dynamics (CFD) in predicting the outcome of BOT is striking. The results suggest a role for CFD in the evaluation of patients for permanent artery occlusion.

The numerical model of the cerebral circulation was utilized along with the data from other supplemental diagnostic modalities to evaluate cerebrocirculatory collateral function during the balloon occlusion test (BOT).

EEG, transcranial Doppler, cerebral oximetry, SPECT, were also done along with the computational modeling for patients undergoing temporary occlusion of the carotid to assess cerebral circulation when permanent occlusion is needed.

Case example: A 49 year old female displayed diplopia and headache. Upon investigation, she was found to have a large right cavernous internal carotid artery (ICA) aneurysm. A computer analysis of her cerebral blood flow was done to assess her cerebral circulation, focusing mainly the total middle cerebral artery flow. The numerical value of the total middle cerebral artery blood flow with and without occlusion of the ipsilateral ICA was predicted by the computer flow to be almost the same.

Vessel	Flow before balloon occlusion	Flow after balloon occlusion
Left Middle cerebral artery and branches	83	81
	40	40
	17	16
	17	16
	16	17
Total MCA Flow	169	172
Right Middle cerebral artery and branches	80	79
	38	35
	18	17
	17	17
	17	15
Total MCA Flow	169	172

In view of the predicted toleration of the occlusion, the patient underwent balloon occlusion of the ICA on the right side, just distal to the aneurysms. The patient displayed good flow in both cerebral hemispheres with minimal changes in total computed middle cerebral artery flow. Concomitantly, there were no change in amplitude in EEG waves, recordings of cerebral oximetry using near infrared spectroscopy, transcranial Doppler (TCD), or clinical deterioration.

Temporary balloon occlusion is invasive and adds risk to the evaluation of patients who may already be at risk for infarction. The numerical model of the cerebral circulation is employed as an aid in the evaluation of patients for permanent internal carotid occlusion.

Pulsatile pressure and flow in normal and diseased vessels (e.g. aneurysms, stenoses) can also be simulated. Modeling of network flow with anatomical variations, bypasses, or lepto-meningeal collateral vessels is also possible.

In this particular case, this model was utilized to simulate changes in the middle cerebral artery blood flow before and after the balloon occlusion. If the blood flow is decreased in a region of the Circle of Willis after occlusion of the carotid artery, the simulation shows red at the region receiving decreased flow, and displays numbers corresponding to the magnitude of the decrease. If the blood flow is increased in a region of the Circle of Willis after occlusion, the simulation shows green at the region receiving increased flow, and denotes the magnitude. From the simulation output, the user can estimate whether the patient will tolerate the occlusion (or would pass the balloon occlusion test).

Further Development of the Model.

Bifurcation.

Flow branching at arterial bifurcations is an important factor in the progression of vascular disease. This blood flow through the artery bifurcation was

extensively studied both by experimental and numerical methods.

Liepsch, *Biorheology*, **21**:571-586 (1984), studied the non-Newtonian fluid in a T-shaped bifurcation. Perktold et al., *Biorheology*, **26**:1011-1030 (1989), studied a Y-shaped bifurcation with an aneurysm in the cerebrovascular tree. Walburn, *J. Biomechanical Engineering*, **104**:66-88 (1982), studied steady flow and pulsatile flow through the aortic bifurcation, secondary flow was not observed during the pulsatile flow but was observed during the steady flow. Fukushima et al., *J. Biomechanical Engineering*, **110**:161-171 (1988), found secondary flow in both steady and pulsatile flow, however, the influence of the secondary flow is smaller during the pulsatile flow than during the steady flow.

To take the importance of the secondary flow into consideration, a few three dimensional computer models have been built. Wille, *J. Biomechanical Engineering*, **6**:49-55 (1984), built a single three-dimensional model of aortic bifurcation with steady flow. Yung et al., *J. Biomechanical Engineering*, **112**:189-297 (1990), studied the steady flow in the aortic bifurcation. In order to generate the mesh conveniently, Yung et al. used a non-physiological area ration of 2.0 to produce flow geometry. Perktold & Peter, *J. Biomechanical Engineering*, **12**:2-12 (1990) studied the wall shear stress in a three-dimensional model of a T-shaped bifurcation. Perktold [*J. Biomechanical Engineering*, **13**:464-475 (1991); *J. Biomechanics*, **24**:409-420 (1991)] analyzed non-Newtonian characteristics, wall shear stress and pulsatile flow in a three-dimensional model of carotid bifurcation. Rindt et al., built a three-

dimensional model for carotid bifurcation, but they used steady flow and rigid vessel wall.

Blood Vessel Wall Elasticity.

The simplest blood vessel wall model is a rigid tube. However vessel wall elasticity has an important effect on the blood flow wave propagation. For a large artery, the vessel wall is composed of three distinct layers, an intima, a media and an adventitia. Each of these layers has a unique function. The vessel wall is not only elastic but also viscoelastic. The vessel elasticity was modeled by a relationship between blood vessel cross-sectional area and local pressure. Raines proposed a widely used model:

$$A(p,x) = A(p_o,x) + \beta \ln(p/p_o) \qquad (4)$$

Another quadratic form used by Porenta, Balar, and Stergiopulos is :

$$A(x) = A_o(x)\left[1 + C_o(p-p_o) + C_o(p-p_o)^2\right] \qquad (5)$$

where β, C'_0 and C'_1 are constants which are determined by experiment.

These models are purely elastic models. However Patel and Vaishnav verified the existence of the viscoelasticity in arterial walls through a dynamic experiment. Reuderink et al. found that neglecting the viscoelasticity of the tube wall could result in an underestimation of both phase velocity and damping. Hawley discovered that a viscoelastic wall model yielded results closer to normal physiological reality than an

elastic wall model. For more discussion about the vessel wall mechanics property, refer to Fung.

Artery Curvature.

In most computer models, arteries were treated as straight tubes. But the structure of the Circle of Willis is three-dimensional, and arteries are bent. Curvature together with pulsatile flow greatly affect wall shear stress and cause secondary flow which may be important in understanding the progression of neurovascular disease. Although curvature was not considered in intracranial cerebral circulation models, blood flow in extracranial curved arteries such as the aortic arch, carotid siphon and coronary arteries were analyzed by a number of researchers. Friedman and Ehrlich digitized the radiography of human aortic bifurcation to obtain the contours of the artery and performed the computation of steady two-dimensional flow in the region. The results suggested that wall slope may be an important factor affecting the variability of shear stress along the medial wall. The variation in the curvature of the proximal iliac entries may affect the susceptibility of these arteries to vascular disease. Chang and Tarbell simulated pulsatile flow in the aortic arch and found that the secondary flow was nearly as large as the axial flow component, the secondary flow was complex with up to seven vortices, peak axial and highest r.m.s. wall shear stress were found at the inside wall. Also the axial-flow direction was reversed at the inside wall.

Chang and Tarbel simulated flow in the coronary artery using the same method of Chang and Tarbel. They found that flow was quasi-steady under resting

conditions but markedly unsteady under exciting conditions. Only a single secondary flow vortex was found. Perktold et al. used two different entrance velocity profiles to study the flow pattern in a slightly curved segment of the left main coronary artery. The different velocity profiles only resulted in significant differences in the immediate vicinity of the inlet, the difference does not persist far into the artery, and significant influence of the secondary flow on the wall shear stress distribution was found.

Perktold et al. analyzed flow in the carotid siphon and left main coronary artery. They found that the maximum secondary flow velocities were on the order of three to four percent of the maximum axial velocity and the secondary flow has an important influence on the wall shear stress distribution.

Some studies of curved arteries include Chandral et al. More general discussion can be found in Pedley.

Non-Newtonian Property of Blood.

It is commonly believed that the blood behaves as a Newtonian fluid in the large blood vessel due to the high shear rate. However, some studies indicated that there were some non-Newtonian effects in the large vessel. It was also found that non-Newtonian effects exist in the low shear area near bends and bifurcations.

Xu used the Casson model to investigate the non-Newtonian effect in artery bifurcation. They found no great differences in velocity profiles. Lou and Yang used a weak-form Casson model to study the non-Newtonian effect in aortic bifurcation. The results indicated that the non-Newtonian property of blood did not drastically change the flow pattern, but caused an

appreciable increase in the shear stress and a slightly higher resistance to both flow separation and the phase shifts between flow layers. Dutta and Tarbell applied a simple power law model in an elastic artery and again found the viscoelasticity of the blood does not appear to influence its flow behavior under physiological conditions in large arteries.

Conclusion

The evolution of models of the cerebral circulation has paralleled the progress in the fields of electrical engineering, fluid dynamics and computer science. With each new possibility of simulation, a closer approach to "physiological" modeling was achieved. The ideal model would be patient specific, highly predictive, and reflective of actual conditions both at the macro and micro circulation level. In addition, such and ideal model would be easily re-configurable to conform with the "real time" demands of clinical medicine.

Although computer models of various degrees of sophistication have been proposed to simulate the cerebral circulation, they have been used mainly as theoretical and research tools. Turning them into tools for clinical applications has the potentially powerful benefit of predicting the result of neurovascular reconstructive procedures. However, none of the published models has ever been validated *in vivo* using quantitative human data, partly because of the lack of available tools for measuring such data.

A specific embodiment of a method and apparatus for modeling cerebral circulation according to the present invention has been described for the purpose of illustrating the manner in which the invention is made

and used. It should be understood that the implementation of other variations and modifications of the invention and its various aspects will be apparent to one skilled in the art, and that the invention is not limited by the specific embodiments described. Therefore, it is contemplated to cover the present invention any and all modifications, variations, or equivalents that fall within the true spirit and scope of the basic underlying principles disclosed and claimed herein.

Claims

WE CLAIM:

1. A method of modeling cerebral circulation in a living subject, such method comprising the steps of:

developing a model for living subjects in general;

correcting the model to substantially conform to the overall cerebral physiology of the living subject; and

calculating a cerebral flow of the living subject based upon the corrected model and a selected cerebral blood flow pertubation.

2. The method of modeling as in claim 1 wherein the step of developing the model further comprises adopting the Circle of Willis.

3. The method of modeling as in claim 1 wherein the step of correcting the model further comprises selecting a vessel of the model.

4. The method of modeling as in claim 3 wherein the step of selecting a vessel of the model further comprises identifying a general area of a corresponding vessel in an image of the living subject.

5. The method of modeling as in claim 4 wherein the step of identifying the corresponding vessel further comprises processing pixel data of the general area of the corresponding vessel to locate a boundary area between the corresponding vessel and surrounding tissue.

6. The method of modeling as in claim 5 wherein the step of processing pixel data of the general area of the corresponding vessel to locate a boundary area between the corresponding vessel and surrounding tissue further comprises measuring a diameter of the corresponding vessel.

7. The method of modeling as in claim 6 wherein the step of processing pixel data of the general area of the corresponding vessel to locate a boundary area between the corresponding vessel and surrounding tissue further comprises tracing the boundary into adjacent areas in three-dimensional space to locate respective ends of the corresponding vessel.

8. The method of modeling as in claim 7 further comprising updating the model based upon the measured diameter and locations of the respective ends of corresponding vessel.

9. The method of modeling as in claim 8 wherein the step of calculating the cerebral flow further comprises using a one-dimensional, explicit, finite difference algorithm based upon a conservation of mass equation.

10. The method of modeling as in claim 9 wherein the step of calculating the cerebral flow further comprises using a Navier-Stokes momentum equation.

11. The method of modeling as in claim 9 wherein the step of calculating the cerebral flow further comprises

using an equation of state relating a local pressure to a local artery size.

12. Apparatus for modeling cerebral circulation in a living subject, such apparatus comprising:

a cerebral circulation model for living subjects in general;

means for correcting the model to substantially conform to the overall cerebral physiology of the living subject; and

means for calculating a cerebral flow of the living subject based upon the corrected model and a selected cerebral blood flow pertubation.

13. The apparatus for modeling as in claim 12 wherein the cerebral circulation model further comprises the Circle of Willis.

14. The apparatus for modeling as in claim 12 wherein the means for correcting the model further comprises means for selecting a vessel of the model.

15. The apparatus for modeling as in claim 14 wherein the means for selecting a vessel of the model further comprises means for identifying a general area of a corresponding vessel in an image of the living subject.

16. The apparatus for modeling as in claim 15 wherein the means for identifying the corresponding vessel further comprises means for processing pixel data of the general area of the corresponding vessel to locate a

boundary area between the corresponding vessel and surrounding tissue.

17. The apparatus for modeling as in claim 16 wherein the means for processing pixel data of the general area of the corresponding vessel to locate a boundary area between the corresponding vessel and surrounding tissue further comprises means for measuring a diameter of the corresponding vessel.

18. The apparatus for modeling as in claim 17 wherein the means for processing pixel data of the general area of the corresponding vessel to locate a boundary area between the corresponding vessel and surrounding tissue further comprises means for tracing the boundary into adjacent areas in three-dimensional space to locate respective ends of the corresponding vessel.

19. The apparatus for modeling as in claim 18 further comprising means for updating the model based upon the measured diameter and locations of the respective ends of corresponding vessel.

20. The apparatus for modeling as in claim 19 wherein the means for calculating the cerebral flow further comprises means using a one-dimensional, explicit, finite difference algorithm based upon a conservation of mass equation.

21. The apparatus for modeling as in claim 20 wherein the means for calculating the cerebral flow further comprises means using a Navier-Stokes momentum equation.

22. The apparatus for modeling as in claim 21 wherein the means for calculating the cerebral flow further comprises means using an equation of state relating a local pressure to a local artery size.

23. Apparatus for modeling cerebral circulation in a living subject, such apparatus comprising:

a cerebral circulation model for living subjects in general;

a correction processor adapted to correct the model to substantially conform to the overall cerebral physiology of the living subject; and

a flow processor adapted to calculate a cerebral flow of the living subject based upon the corrected model and a selected cerebral pertubation.

24. The apparatus for modeling as in claim 23 wherein the cerebral circulation model further comprises the Circle of Willis.

25. The apparatus for modeling as in claim 23 wherein the correction processor further comprises a cursor adapted to select a vessel of the model.

26. The apparatus for modeling as in claim 25 wherein the correction processor further comprises a pixel processor adapted to process pixel data of the general area of the corresponding vessel to locate a boundary area between the corresponding vessel and surrounding tissue.

27. The apparatus for modeling as in claim 26 wherein the pixel processor further comprises a distance processor adapted to measure a diameter of the corresponding vessel.

28. The apparatus for modeling as in claim 27 wherein the pixel processor further comprises a tracing processor adapted to trace the boundary into adjacent areas in three-dimensional space to locate respective ends of the corresponding vessel.

29. A method of modeling a surgical alteration of cerebral circulation in a living human subject, such method comprising the steps of:

developing a model for living subjects in general;

correcting the model to substantially conform to the cerebral physiology of the living subject;

perturbing the corrected model; and

determining a set of flow changes occurring as a result of the perturbation.

30. The method of modeling as in claim 29 wherein the step of developing the model further comprises adopting the Circle of Willis.

31. The method of modeling as in claim 29 wherein the step of correcting the model further comprises selecting a vessel of the model.

32. The method of modeling as in claim 31 wherein the step of selecting a vessel of the model further

comprises identifying a general area of a corresponding vessel in an image of the living subject.

33. The method of modeling as in claim 32 wherein the step of identifying the corresponding vessel further comprises processing pixel data of the general area of the corresponding vessel to locate a boundary area between the corresponding vessel and surrounding tissue.

34. The method of modeling as in claim 33 wherein the step of processing pixel data of the general area of the corresponding vessel to locate a boundary area between the corresponding vessel and surrounding tissue further comprises measuring a diameter of the corresponding vessel.

35. The method of modeling as in claim 34 wherein the step of processing pixel data of the general area of the corresponding vessel to locate a boundary area between the corresponding vessel and surrounding tissue further comprises tracing the boundary into adjacent areas in three-dimensional space to locate respective ends of the corresponding vessel.

36. The method of modeling as in claim 35 further comprising updating the model based upon the measured diameter and locations of the respective ends of corresponding vessel.

37. The method of modeling as in claim 36 wherein the step of calculating the cerebral flow further comprises

using a one-dimensional, explicit, finite difference algorithm based upon a conservation of mass equation.

38. The method of modeling as in claim 38 wherein the step of calculating the cerebral flow further comprises using a Navier-Stokes momentum equation.

39. The method of modeling as in claim 38 wherein the step of calculating the cerebral flow further comprises using an equation of state relating a local pressure to a local artery size.

40. Apparatus for modeling a surgical alteration of cerebral circulation in a living human subject, such apparatus comprising:

a cerebral model for living subjects in general;

means for correcting the model to substantially conform to the cerebral physiology of the living subject;

means for perturbing the corrected model; and

means for determining a set of flow changes occurring as a result of the perturbation.

41. The apparatus for modeling as in claim 40 wherein the means for correcting the model further comprises means for selecting a vessel of the model.

42. The apparatus for modeling as in claim 41 wherein the means for selecting a vessel of the model further comprises means for identifying a general area of a corresponding vessel in an image of the living subject.

43. The apparatus for modeling as in claim 42 wherein the means for identifying the corresponding vessel further comprises means for processing pixel data of the general area of the corresponding vessel to locate a boundary area between the corresponding vessel and surrounding tissue.

44. The apparatus for modeling as in claim 43 wherein the means for processing pixel data of the general area of the corresponding vessel to locate a boundary area between the corresponding vessel and surrounding tissue further comprises means for measuring a diameter of the corresponding vessel.

45. The apparatus for modeling as in claim 44 wherein the means for processing pixel data of the general area of the corresponding vessel to locate a boundary area between the corresponding vessel and surrounding tissue further comprises means for tracing the boundary into adjacent areas in three-dimensional space to locate respective ends of the corresponding vessel.

46. The apparatus for modeling as in claim 45 further comprising means for updating the model based upon the measured diameter and locations of the respective ends of corresponding vessel.

47. The apparatus for modeling as in claim 46 wherein the means for calculating the cerebral flow further comprises means using a one-dimensional, explicit, finite difference algorithm based upon a conservation of mass equation.

48. The apparatus for modeling as in claim 47 wherein the means for calculating the cerebral flow further comprises means using a Navier-Stokes momentum equation.

49. The apparatus for modeling as in claim 48 wherein the means for calculating the cerebral flow further comprises means using an equation of state relating a local pressure to a local artery size.

50. A method of modeling a surgical alteration of circulation in a predetermined region of a living human subject, such method comprising the steps of:

developing a model of the region for living subjects in general;

correcting the model to substantially conform to the physiology of the region of the living subject;

perturbing the corrected model; and

determining a set of flow changes occurring as a result of the perturbation.

FIG. 1

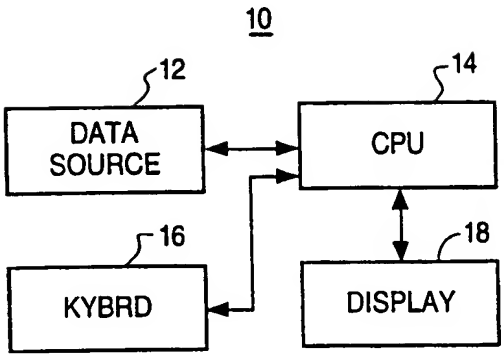

FIG. 2

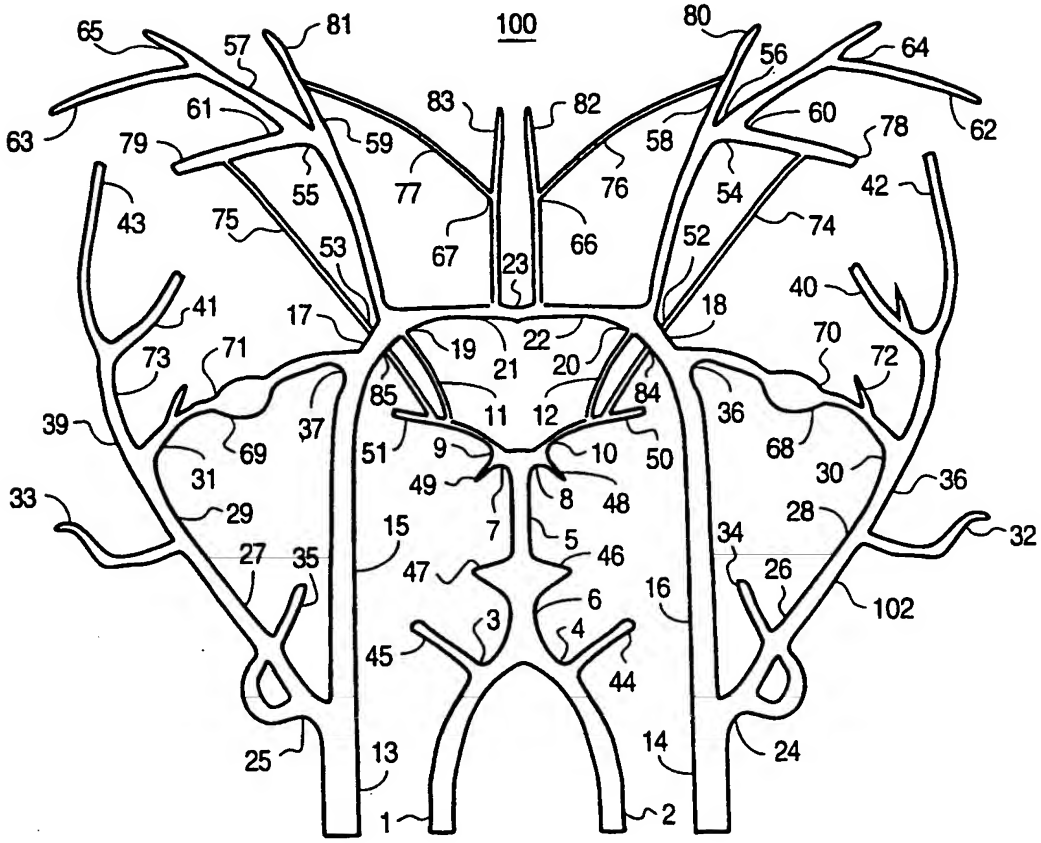

FIG. 3

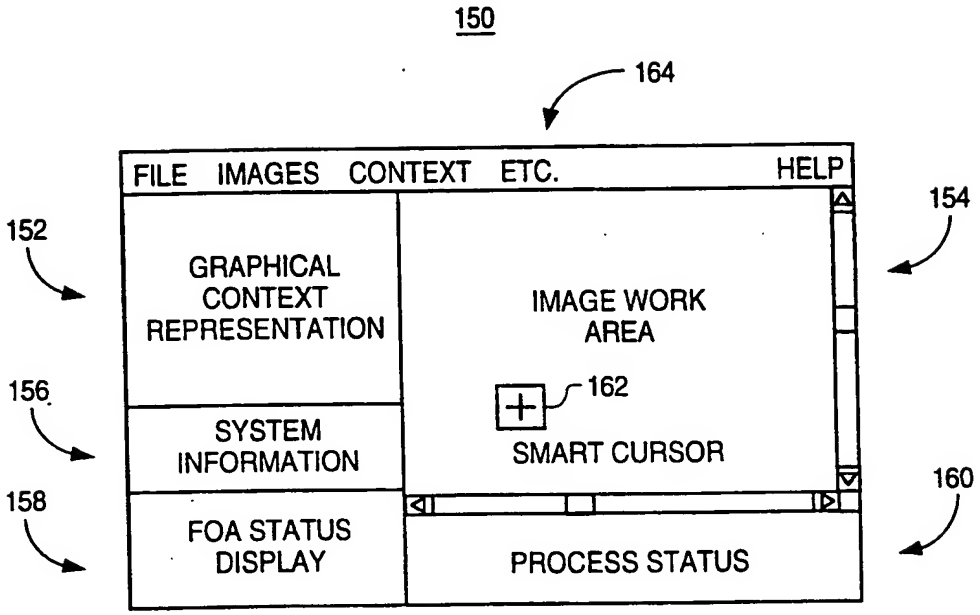

FIG. 4

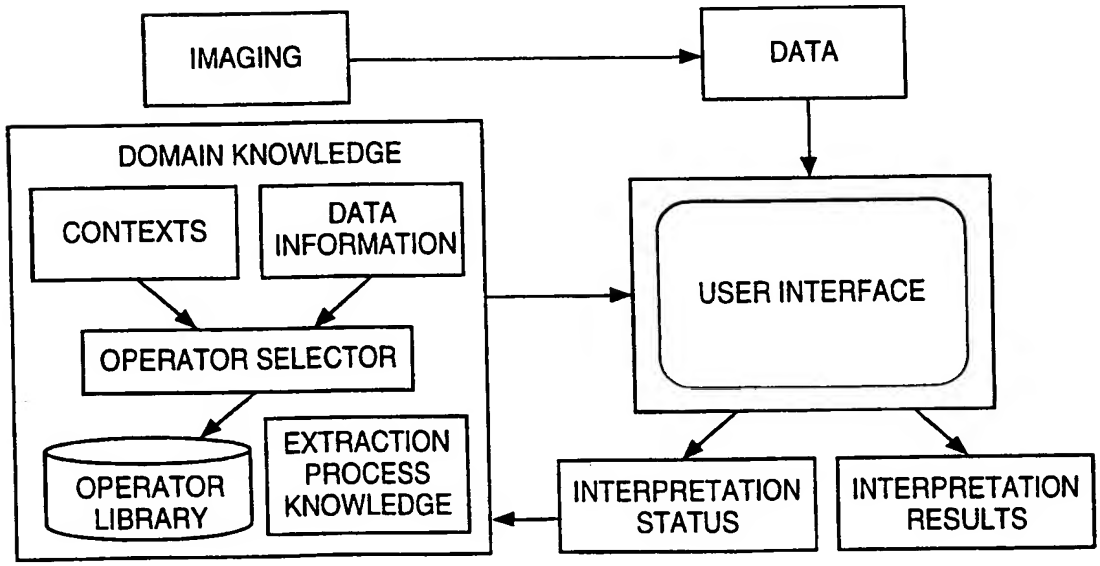

FIG. 5

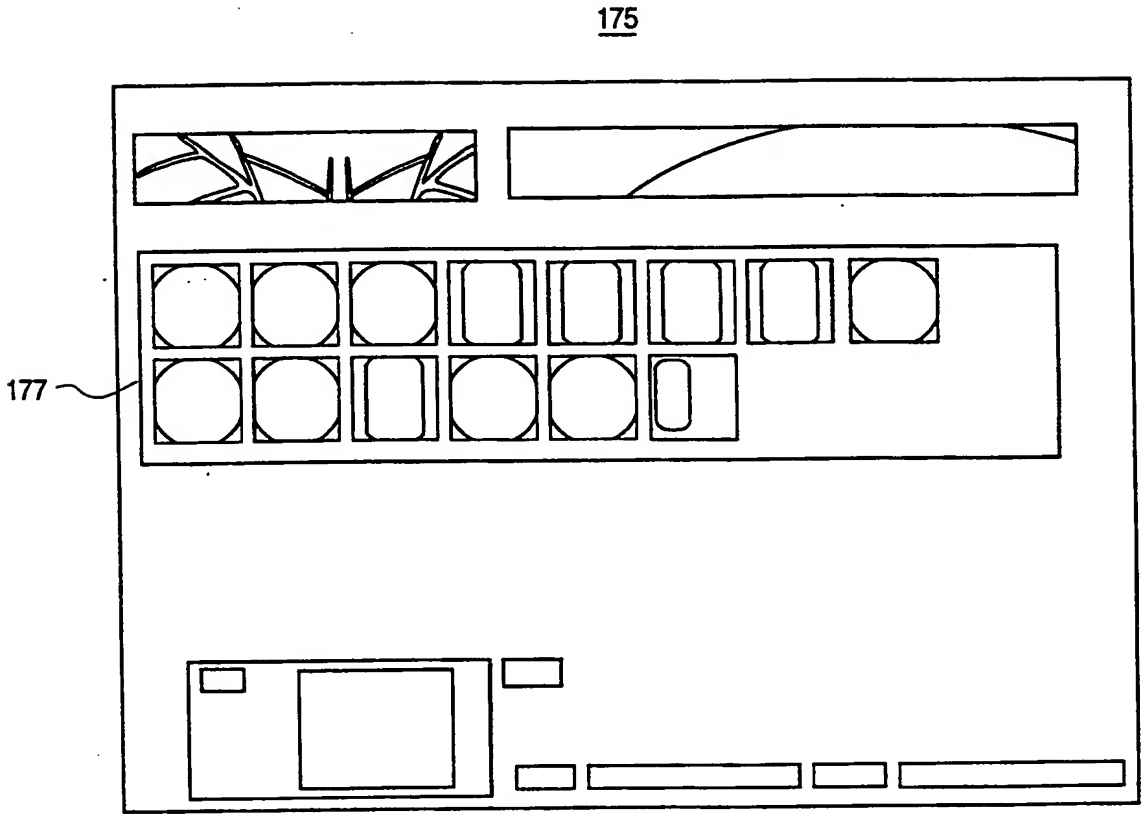

FIG. 6

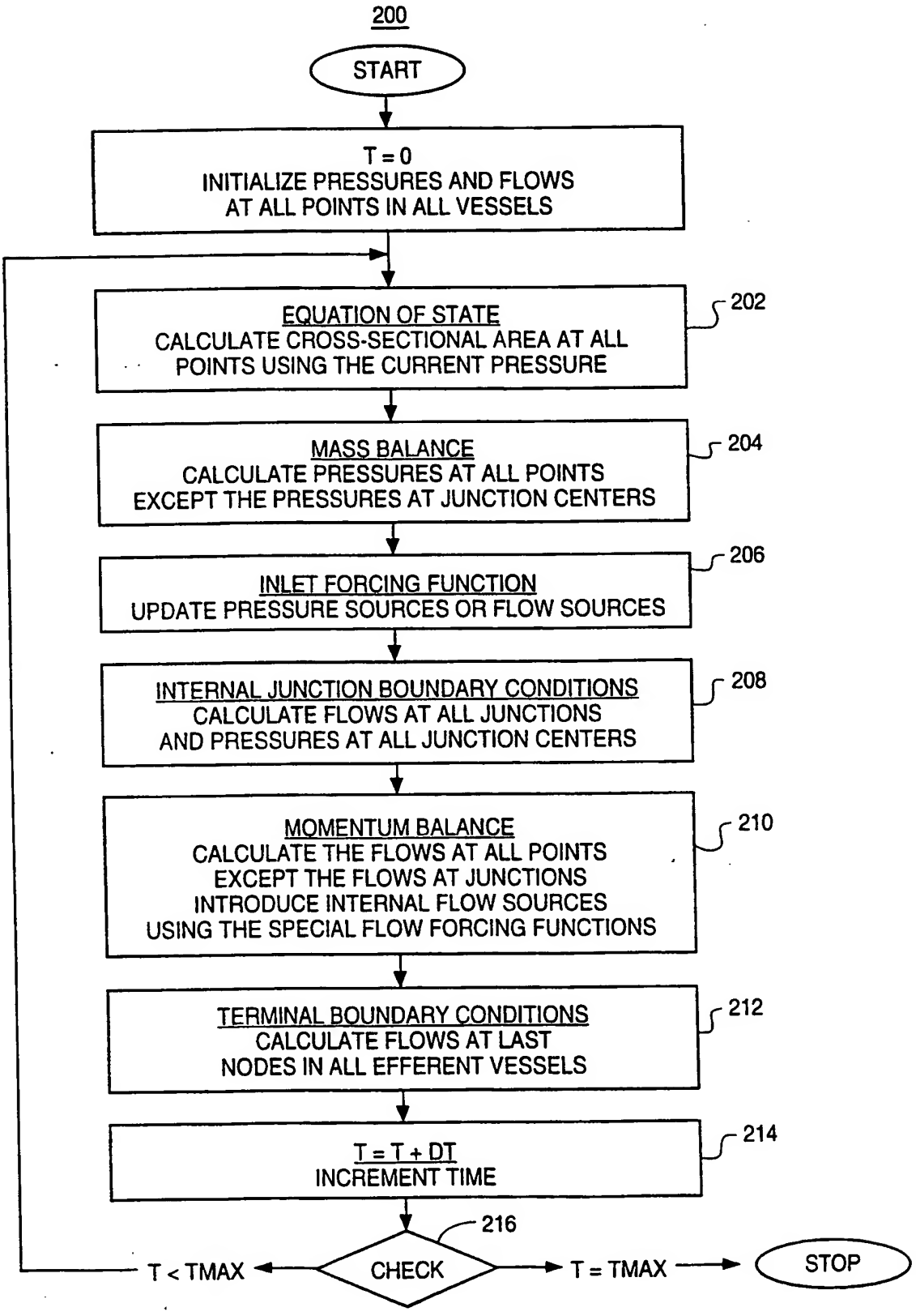

FIG. 7

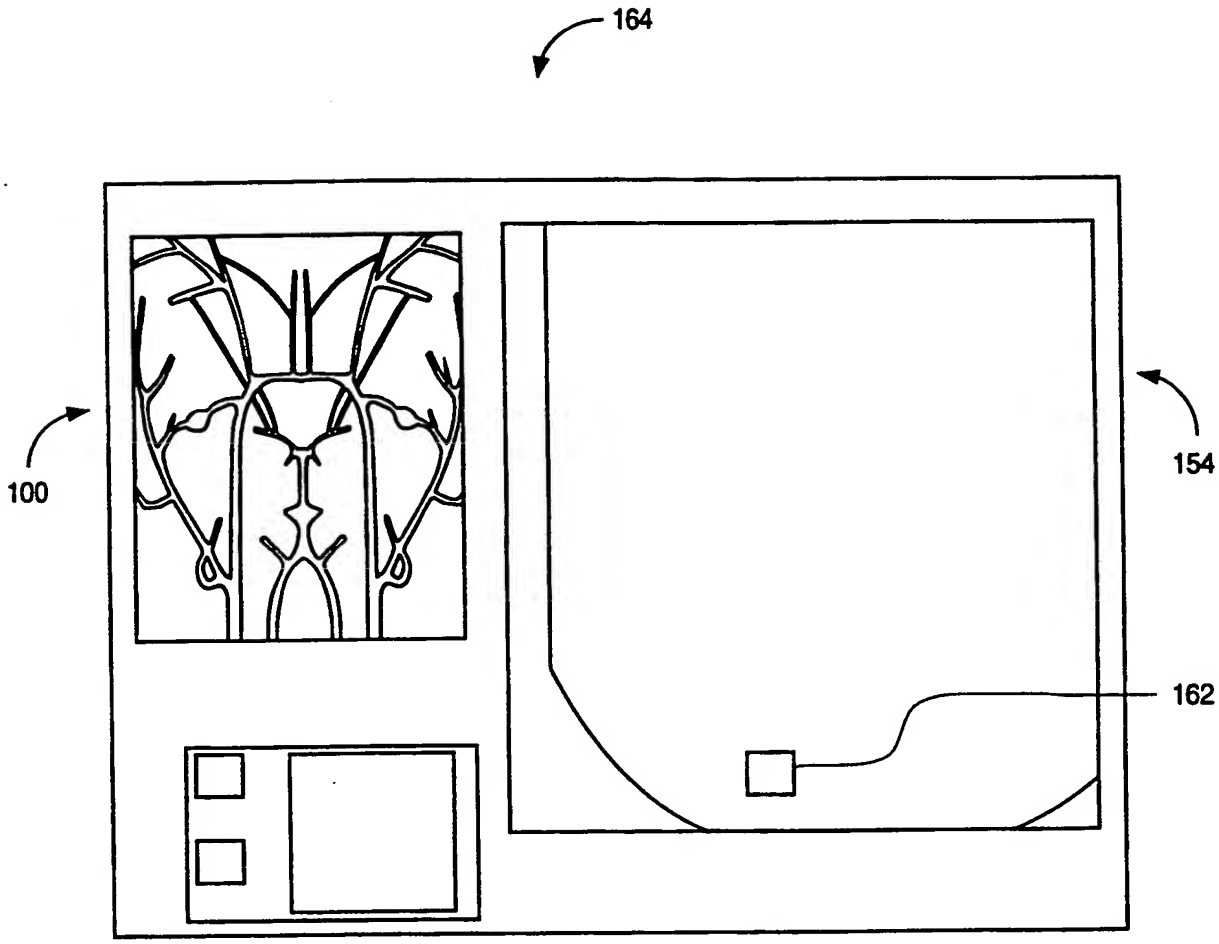

AIM NEUROVASCULAR INTERPRETATION SYSTEM INTERFACE

INTERNATIONAL SEARCH REPORT

International application No.
PCT/US99/02276

A. CLASSIFICATION OF SUBJECT MATTER

IPC(6) :A61B 05/00
US CL :600/407

According to International Patent Classification (IPC) or to both national classification and IPC

B. FIELDS SEARCHED

Minimum documentation searched (classification system followed by classification symbols)

U.S. : 128/920, 922, 924; 382/128, 130; 364/224.3, 224.6, 275.6, 275.7, 922, 922.2-922.4; 395/924; 600/407, 410, 416, 419

Documentation searched other than minimum documentation to the extent that such documents are included in the fields searched

Electronic data base consulted during the international search (name of data base and, where practicable, search terms used)

C. DOCUMENTS CONSIDERED TO BE RELEVANT

Category*	Citation of document, with indication, where appropriate, of the relevant passages	Relevant to claim No.
Y --- A	US 5,273,038 A (BEAVIN) 28 December 1993, see Abstract, column 1 lines 34-61, column 3 line 67 to column 4 line 18, column 5 lines 7-17, column 6 lines 29-50, column 7 lines 1-36, and claims 1-11.	1-8, 12-19, 23-27, 29-34, 40-44, 50 --- 9-11, 20-22, 28, 35-39, 45-49

[X] Further documents are listed in the continuation of Box C. [ ] See patent family annex.

* Special categories of cited documents:

"A" document defining the general state of the art which is not considered to be of particular relevance

"E" earlier document published on or after the international filing date

"L" document which may throw doubts on priority claim(s) or which is cited to establish the publication date of another citation or other special reason (as specified)

"O" document referring to an oral disclosure, use, exhibition or other means

"P" document published prior to the international filing date but later than the priority date claimed

"T" later document published after the international filing date or priority date and not in conflict with the application but cited to understand the principle or theory underlying the invention

"X" document of particular relevance; the claimed invention cannot be considered novel or cannot be considered to involve an inventive step when the document is taken alone

"Y" document of particular relevance; the claimed invention cannot be considered to involve an inventive step when the document is combined with one or more other such documents, such combination being obvious to a person skilled in the art

"&" document member of the same patent family

Date of the actual completion of the international search

03 JUNE 1999

Date of mailing of the international search report

18 JUN 1999

Name and mailing address of the ISA/US
Commissioner of Patents and Trademarks
Box PCT
Washington, D.C. 20231

Facsimile No. (703) 305-3230

Authorized officer

SHAWNA J. SHAW

Telephone No. (703) 308-2985

Form PCT/ISA/210 (second sheet)(July 1992)★

INTERNATIONAL SEARCH REPORT

International application No.
PCT/US99/02276

C (Continuation). DOCUMENTS CONSIDERED TO BE RELEVANT

Category*	Citation of document, with indication, where appropriate, of the relevant passages	Relevant to claim No.
Y --- A	US 5,603,322 A (JEŞMANOWICZ et al.) 18 February 1997, Astract, Figs. 6 and 7, column 2 lines 41-60, column 6 lines 42-57, and column 13 lines 14-18.	1-8, 12-19, 23-27, 29-34, 40-44, 50 --- 9-11, 20-22, 28, 35-39, 45-49
Y ---P A	US 5,833,610 A (YOKAWA et al.) 10 November 1998, Abstract, Fig. 3, column 1 lines 6-59, column 2 lines 20-25, and claims 1 and 2.	1-8, 12-19, 23-27, 29-34, 40-44, 50 --- 9-11, 20-22, 28, 35-39, 45-49
A, P	US 5,812,691 A (UDUPA et al.) 22 September 1998, Abstract, Figs. 1-4, and claims 1 and 13.	1-50
A, P	US 5,768,405 A (MAKRAM-EBEID) 16 June 1998, Abstract, Figs. 3 and 10, and claims 1 and 2.	1-50
A, P	US 5,852,646 A (KLOTZ et al.) 22 December 1998, Abstract, Figs. 1 and 2, and claims 1 and 8.	1-50